INTERNATIONAL JOURNAL FOR NUMERICAL METHODS IN FLUIDS, VOL. 8, 65–79 (1988)

A BOUNDARY-TYPE FINITE ELEMENT MODEL FOR WATER SURFACE WAVE PROBLEMS

KAZUO KASHIYAMA*

Department of Civil Engineering, Hiroshima Institute of Technology, Miyake, Itsukaichi, Saeki-ku, Hiroshima 731–51, Japan

MUTSUTO KAWAHARA†

Department of Civil Engineering, Chuo University, Kasuga, Bunkyo-ku, Tokyo 112, Japan

SUMMARY

A new combinative method of boundary-type finite elements and boundary solutions is presented to study wave diffraction–refraction and harbour oscillation problems. The numerical model is based on the mild-slope equation. The key feature of this method is that the discretized matrix equation can be formulated only by the calculation of a line integral, since the interpolation equation which satisfies the governing equation in each element is used. The numerical solutions are compared with existing analytical, experimental, observed and other numerical results. The present method is shown to be an effective and accurate method for water surface wave problems.

KEY WORDS Boundary-type finite element method Mild-slope equation Wave diffraction–refraction Harbour oscillation C_0 non-conforming element

INTRODUCTION

The demands of the planning and construction of various offshore and coastal structures have increased in recent years. Consequently, the analysis of wave diffraction–refraction problems and harbour oscillation problems is becoming more important from the point of view of the planning of offshore and coastal structures. Various numerical methods have been presented to analyse water surface wave problems. The eigen function expansion method,[1,2] the finite difference method,[3] the finite element method[4] and the boundary element method[5–9] have been developed. However, the finite difference method and the finite element method have difficulty in considering the Sommerfeld radiation condition. Recently, some combinative methods based on the finite element method have also been developed to overcome this difficulty, since the finite element method can easily treat the arbitrary shape and variable water depth. These combinative methods are roughly classified into three types with respect to the treatment of the radiation condition. Chen and Mei,[10] Zienkiewicz *et al.*,[11] Houston,[12] Tsay and Liu[13] and Skovgaard *et al.*[14] presented the combinative method of finite elements and boundary solutions. This method is called the hybrid finite element method. Berkhoff[15,16] and Zienkiewicz *et al.*[17] presented the combinative method using boundary elements. Battess and Zienkiewicz,[18] Bettess *et al.*[19,20] and Zienkiewicz *et al.*[21] presented the combinative method using infinite elements. However, the principal objective of these methods was

* Research associate.
† Professor.

0271–2091/88/010065–15$07.50

Received 28 March 1986

how to treat the radiation condition rationally in the computation rather than the improvement of solutions in the finite element region. More recently, the present authors[22–24] presented a new finite element method which is more accurate than the conventional finite element method. This method introduced the concept of the boundary element method and is referred to as the boundary-type finite element method.

This paper presents a new combinative method based on the boundary-type finite element method. The key feature of this method is that the discretized matrix equation can be formulated only by the calculation of a line integral, since the interpolation equation which satisfies the governing equation in each element is used. The mild-slope equation is employed for the governing equation. This equation reduces a three-dimensional problem to a two-dimensional problem where the water depth is assumed to be slowly varying in space. Futhermore, this equation is applicable to a wide range of wave frequency. The present method has been applied to wave diffraction–refraction by island and offshore structures and to harbour oscillation problems. The computed results are compared with existing analytical, experimental, observed and other numerical solutions.

BASIC EQUATIONS

Consider a wave field as shown in Figure 1. Assuming steady state surface waves with infinitesimal amplitude on a slowly varying water depth, the surface displacement η may be described by the mild-slope equation[15,25–27]

$$\nabla\cdot(CC_g\nabla\eta)+\omega^2\frac{C_g}{C}\eta=0 \quad \text{in} \quad \Omega, \tag{1}$$

where C is the phase velocity, C_g is the group velocity and ω is the angular frequency. These characteristic values are determined by the dispersion relation

$$\omega^2=gk\tanh kh, \tag{2}$$

where g is the gravitational acceleration, k is the wave number and h is the water depth.

The following conditions are introduced on the boundary:

$$\eta_{,n}=\partial\eta/\partial n=0 \quad \text{on} \quad \Gamma_s, \tag{3}$$

$$\lim_{r\to\infty} r^{1/2}(\eta_{sc,r}-ik\eta_{sc})=0 \quad \text{on} \quad \Gamma_\infty, \tag{4}$$

where n means the normals to the boundary, r is the distance from structures, i is the imaginary

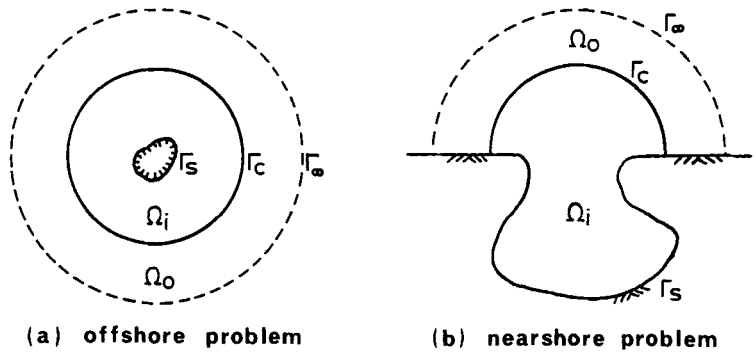

(a) offshore problem (b) nearshore problem

Figure 1. Definition of offshore and nearshore problems

unit, η_{sc} is the scattered wave, Γ_s is the boundary of the coastline and Γ_∞ is the infinite boundary.

The wave field Ω is divided into two domains: the inner domain Ω_i with variable water depth and the outer domain Ω_0 with constant water depth. On the boundary of Γ_c, the following continuity conditions should be satisfied:

$$\left.\begin{aligned} \eta &= \bar{\eta} \\ \eta_{,n} &= \bar{\eta}_{,n} \end{aligned}\right\} \quad \text{on} \quad \Gamma_c, \tag{5}$$

where $\bar{\eta}$ denotes the surface displacement within the outer domain.

Two cases are considered (Figure 1): offshore problems and nearshore problems. In the case of offshore problems, the surface displacement η is assumed to be the sum of the incident wave η_{in} and scattered wave η_{sc}:

$$\eta = \eta_{in} + \eta_{sc}, \tag{6}$$

where η_{in} is given by

$$\eta_{in} = A \sum_{n=0}^{\infty} \varepsilon_n i^n J_n(kr) \cos n(\theta - \theta_{in}), \tag{7}$$

in which A denotes incident wave amplitude, ε_n is the Neumann number, J_n is the Bessel function of order n and θ_{in} is the incident wave angle.

On the other hand, in the case of nearshore problems, the surface wave displacement is assumed as follows:

$$\eta = \eta_{in} + \eta_{re} + \eta_{sc}, \tag{8}$$

where

$$\eta_{in} + \eta_{re} = 2A \sum_{n=0}^{\infty} \varepsilon_n i^n J_n(kr) \cos n\theta_{in} \cos n\theta, \tag{9}$$

in which η_{re} denotes the reflected wave displacement.

COMBINATIVE METHOD USING BOUNDARY-TYPE FINITE ELEMENTS[22-24]

For efficient numerical computation, the boundary-type finite element method is employed in the inner domain Ω_i and the boundary solution method, first presented by Chen and Mei,[10] is introduced in the outer domain Ω_0 to deal with the radiation condition.

The scattered wave within the outer domain, $\bar{\eta}_{sc}$, must satisfy the Helmholtz equation and the radiation condition. In the case of offshore problems, as shown in Figure 1(*a*), the scattered wave can be represented by the Fourier–Bessel expansion as

$$\bar{\eta}_{sc} = \alpha_0 H_0(kr) + \sum_{n=1}^{\infty} H_n(kr)(\alpha_n \cos n\theta + \beta_n \sin n\theta), \tag{10}$$

where α_n and β_n denote the unknown constants and H_n is the Hankel function of the first kind of order n.

On the other hand, in the case of nearshore problems, as shown in Figure 1(*b*), the scattered wave can be represented as

$$\bar{\eta}_{sc} = \sum_{n=0}^{\infty} \alpha_n H_n(kr) \cos n\theta, \tag{11}$$

where α_n denotes the unknown constants.

For the discretization of the spatial variable η, the variational principle can be introduced in the formulation. The variational function to be minimized for the given boundary value problem is expressed as

$$\Pi = \Pi_i + \Pi_o, \tag{12}$$

where

$$\Pi_i = \tfrac{1}{2}\int_{\Omega_i}\left(CC_g(\nabla\eta)^2 - \omega^2\frac{C_g}{C}\eta^2\right)d\Omega,$$

$$\Pi_o = \int_{\Gamma_c} CC_g[(\tfrac{1}{2}\bar{\eta}_{sc} - \eta_{sc})\bar{\eta}_{,n} - \tfrac{1}{2}\bar{\eta}_{sc}\eta_{ir,n}]\,d\Gamma,$$

in which Π_i and Π_o are the variational functions of the inner and outer domain respectively and η_{ir} denotes the sum of the incident and reflected waves.

The wave field in the finite element region is divided into a finite number of elements, and the variational function of Π_i can be written as

$$\Pi_i = \sum_{e=1}^{Ne}\left[\tfrac{1}{2}\int_{\Omega_{ie}}\left(CC_g(\nabla\eta)^2 - \omega^2\frac{C_g}{C}\eta^2\right)d\Omega\right], \tag{13}$$

where e denotes the eth finite element and Ne is the total number of elements. Integrating the first term by parts and introducing the relation $\omega = Ck$, the variational function can be transformed into the form

$$\Pi_i = \sum_{e=1}^{Ne}\left(\tfrac{1}{2}\int_{\Gamma_{ie}} CC_g\eta\eta_{,n}\,d\Gamma - \tfrac{1}{2}\int_{\Omega_{ie}} CC_g\eta(\nabla^2\eta + k^2\eta)\,d\Omega\right), \tag{14}$$

where Γ_{ie} denotes the boundary of eth finite element. Assuming that the interpolation equation for surface displacement satisfies the Helmholtz equation in each finite element, the variational function can be formulated only by the line integral as follows:

$$\Pi_i = \sum_{e=1}^{Ne}\left(\tfrac{1}{2}\int_{\Gamma_{ie}} CC_g\eta\eta_{,n}\,d\Gamma\right). \tag{15}$$

For the interpolation equation, a trigonometric function series is employed based on a three-node triangular element:

$$\eta = \left[\cos\left(\frac{k}{\sqrt{2}}x\right)\cos\left(\frac{k}{\sqrt{2}}y\right)\quad \cos\left(\frac{k}{\sqrt{2}}x\right)\sin\left(\frac{k}{\sqrt{2}}y\right)\quad \sin\left(\frac{k}{\sqrt{2}}x\right)\cos\left(\frac{k}{\sqrt{2}}y\right)\right]\begin{Bmatrix}\gamma_1\\ \gamma_2\\ \gamma_3\end{Bmatrix}, \tag{16}$$

where γ_1, γ_2 and γ_3 are constants and k is the wave number which takes the mean value of each element. This interpolation equation satisfies the Helmholtz equation. Figure 2 shows typical forms of the interpolation function in cases where the ratio between the element length s and the

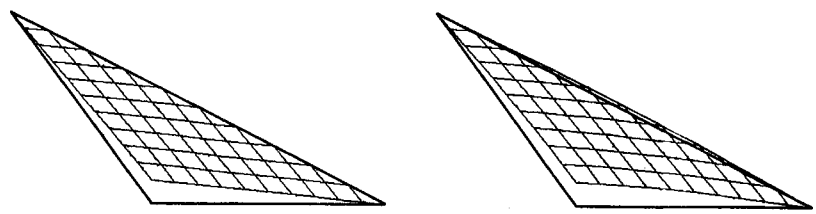

Figure 2. Typical form of the interpolation function

wavelength L is 0·1 and 0·33. From this figure, it can be seen that the shape of the interpolation function varies according to the value of the wave number and the boundary-type finite element is the C_0 non-conforming element. The value of CC_g is approximated by using linear interpolation.

Introducing the interpolation equation (16) into (15) and integrating the term, equation (15) can be written in matrix form:[22–24]

$$\Pi_i = \tfrac{1}{2}\{\eta\}^T[\mathbf{K}_1]\{\eta\}, \tag{17}$$

where $[\mathbf{K}_1]$ denotes the global stiffness matrix.

On the other hand, the variational function in the outer domain can be expressed as

$$\begin{aligned}\Pi_o &= \int_{\Gamma_c} CC_g[(\tfrac{1}{2}\bar{\eta}_{sc} - \eta_{sc})(\bar{\eta}_{sc,n} + \eta_{ir,n}) - \tfrac{1}{2}\bar{\eta}_{sc}\eta_{ir,n}]\,d\Gamma \\ &= \tfrac{1}{2}\int_{\Gamma_c} CC_g\bar{\eta}_{sc}\bar{\eta}_{sc,n}\,d\Gamma - \int_{\Gamma_c} CC_g\eta\bar{\eta}_{sc,n}\,d\Gamma - \int_{\Gamma_c} CC_g\eta\eta_{ir,n}\,d\Gamma \\ &\quad + \int_{\Gamma_c} CC_g\eta_{ir}\bar{\eta}_{sc,n}\,d\Gamma + \int_{\Gamma_c} CC_g\eta_{ir}\eta_{ir,n}\,d\Gamma. \end{aligned} \tag{18}$$

For simplicity, the boundary of Γ_c is assumed to be a circle; then the integral of the first term can be evaluated analytically. The boundary of Γ_c is divided into a finite number of line segments and linear interpolation is employed for the interpolation of surface displacement. Finally, equation (18) can be written as[10,26]

$$\Pi_o = \tfrac{1}{2}\{\mu\}^T[\mathbf{K}_2]\{\mu\} + \{\hat{\eta}\}^T[\mathbf{K}_3]\{\mu\} - \{Q_1\}^T\{\hat{\eta}\} - \{Q_2\}^T\{\mu\}, \tag{19}$$

where $\{\mu\}$ denotes the unknown constant in the expansion of the outer domain and $\{\hat{\eta}\}$ is the surface displacement of the nodal point on the boundary Γ_c.

Summarizing, the variational function to be minimized can be written in the form

$$\begin{aligned}\Pi &= \Pi_i + \Pi_o \\ &= \tfrac{1}{2}\{\eta\}^T[\mathbf{K}_1]\{\eta\} + \tfrac{1}{2}\{\mu\}^T[\mathbf{K}_2]\{\mu\} + \{\hat{\eta}\}^T[\mathbf{K}_3]\{\mu\} - \{Q_1\}^T\{\hat{\eta}\} - \{Q_2\}^T\{\mu\}. \end{aligned} \tag{20}$$

Minimizing (20) gives

$$\partial\Pi/\partial\eta_i = 0, \quad i = 1, 2, \ldots, E, \tag{21}$$

$$\partial\Pi/\partial\mu_i = 0, \quad i = 1, 2, \ldots, M, \tag{22}$$

where E and M are the total number of nodal points and the total number of coefficients in the expansion of the outer domain, respectively. From equations (21) and (22), a set of linear complex algebraic equations for $\{\eta\}$ and $\{\mu\}$ is obtained:

$$[\mathbf{K}_1]\{\eta\} + [\mathbf{K}_3]\{\mu\} = \{Q_1\}, \tag{23}$$

$$[\mathbf{K}_2]\{\mu\} + [\mathbf{K}_3]^T\{\hat{\eta}\} = \{Q_2\}, \tag{24}$$

where $[\mathbf{K}_1]$ is the tridiagonal matrix of E by E, $[\mathbf{K}_2]$ is the diagonal matrix of M by M and $[\mathbf{K}_3]$ is the full matrix of P by M; here P is the total number of nodal points on the boundary Γ_c. Eliminating the constants $\{\mu\}$, the matrix equation for $\{\eta\}$ can be derived in the form

$$[\mathbf{K}]\{\eta\} = \{Q\}, \tag{25}$$

where $[\mathbf{K}]$ is the symmetric matrix. The band matrix method is used to solve equation (25).

NUMERICAL EXAMPLES

In order to show the validity and efficiency of the present combinative method, several computations have been carried out and compared with the analytical, experimental and observed results. The total number of coefficients in the expansion of the outer domain is assumed to be $n = 10$ for all computations in this paper.

Offshore problems

First, the classical Homma island[28,29] is considered, as shown in Figure 3. The present method is applied to the analysis of the wave amplitude distribution around a circular island on a parabolic shoal. The exact solution for this problem have been obtained by Jonsson *et al.*[30] Figure 4 shows the finite element idealization and computed wave amplitude distribution for as incident wave period of 480 s. The total numbers of finite elements and nodal points are 720 and 396 respectively. The incident wave angle is assumed to be $\theta_{in} = 0°$. Table 1 shows the difference between exact and

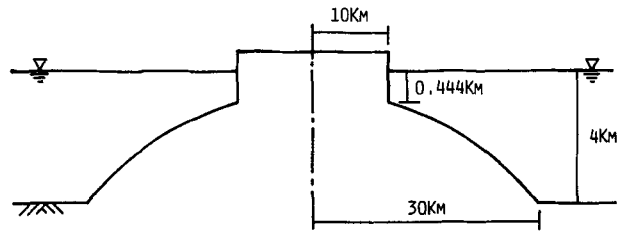

Figure 3. Circular island on a parabolic shoal

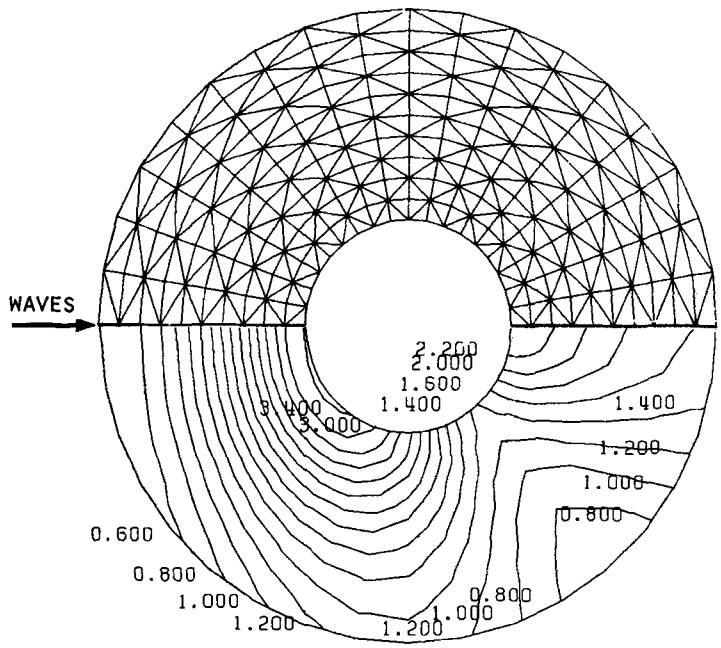

Figure 4. Finite element idealization and computed relative wave amplitude when the incident wave period is 8 min

Table 1. Comparison of computed relative wave amplitude and phase function

	Method	$\theta = 0°$	$\theta = 30°$	$\theta = 60°$	$\theta = 90°$	$\theta = 120°$	$\theta = 150°$	$\theta = 180°$	$\Sigma\|\text{line}\|$
Amplitude	Exact	2·3708	1·7663	1·5067	2·6885	3·3686	3·4553	3·4193	
	FEM	−0·1118	−0·0373	−0·0167	−0·0625	−0·0886	−0·0193	−0·0333	0·3695
	BFEM	+0·0242	+0·0297	+0·0083	+0·0095	+0·0034	+0·0037	+0·0077	0·0865
Phase	Exact	151·69	134·42	60·33	16·40	355·95	341·70	335·92	
	FEM	−3·81	−3·96	−1·14	−1·10	−1·34	−1·12	−0·84	13·31
	BFEM	−0·66	−0·29	+1·26	+0·90	+1·19	+1·80	+2·14	8·24

computed results for the relative wave amplitude and phase function along the coastline. In this table, Exact denotes the exact solution, FEM the conventional method using conforming linear triangular elements and BFEM the present method. For FEM solutions, the maximum amplitude error is 0·1118 at $\theta = 0°$, which corresponds to 4·72%, the relative mean error is 2·06% and the relative mean error of phase is 1·90°. On the other hand, for BFEM solutions, the maximum amplitude error is 0·0297 at $\theta = 30°$, which corresponds to 1·68%, the relative mean error is 0·58% and the relative mean error of phase is 1·18°. From Table 1, it can be seen that the present method is in better agreement with the exact solution than is the conventional method, particularly at the rear side of the island.

Second, an elliptic island on a circular base is considered, as shown in Figure 5. Figure 6 shows the finite element idealization for an elliptic island. The total numbers of finite elements and nodal points are 288 and 180 respectively. The bottom slope violates the mild-slope assumption. The computed results of the relative wave amplitude and phase function along the coastline are compared with the 3D finite element solutions obtained by Yue *et al.*[31] Figures 7 and 8 illustrate the comparison when the incident wave angle is $\theta_{in} = 180°$ and $\theta_{in} = 270°$ respectively. The incident wave number is assumed to be $ka = 1·0$. The maximum error is roughly 10%. The discrepancies could be attributed to the violation of the mild-slope assumption. However, these results are acceptable in terms of the accuracy requirements of many engineering applications.

Nearshore problems

The present method is applied to harbour oscillation problems. To test the present method, a rectangular harbour of dimensions $2h$ long by h wide by h deep, where h is the water depth, is considered, as shown in Figure 9, which was first studied by Mattioli.[7] Figures 9 and 10 show the finite element idealization and water depth diagram for the rectangular harbour. The total numbers of finite elements and nodal points are 116 and 80 respectively. Figure 11 illustrates the computed relative wave amplitude at the centre of the backwall (point P) versus kh for a constant water depth (Figure 10(*a*)). The computed results are well in agreement with the exact solution obtained by Mattioli.

To test the present method further, it is applied to a harbour with a slowly varying water depth (Figure 10(*b*)). Figure 12 shows the computed relative wave amplitude at the point P, compared with the existing experimental and other numerical results. In this figure, the full curve represents the computed results obtained by the present method, the broken curve represents the 2D boundary element solution by Mattioli and the chain curve and full circles are the 3D boundary element solution and experimental results by Yoshida and Ijima.[32] The experimental results are measured at point M using capacity-type wave gauges. The 2D boundary element solutions are different from the other numerical and experimental results, since the shallow water theory is used

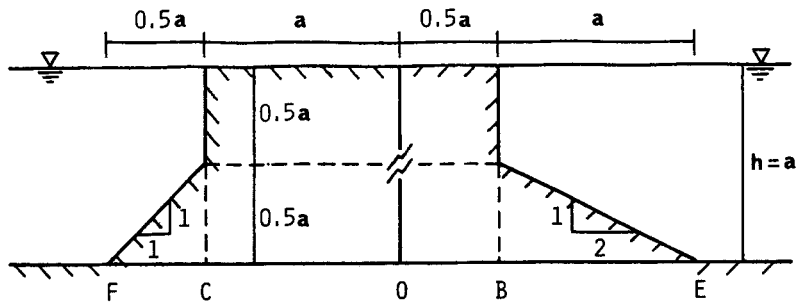

Figure 5. Elliptic island on a circular base

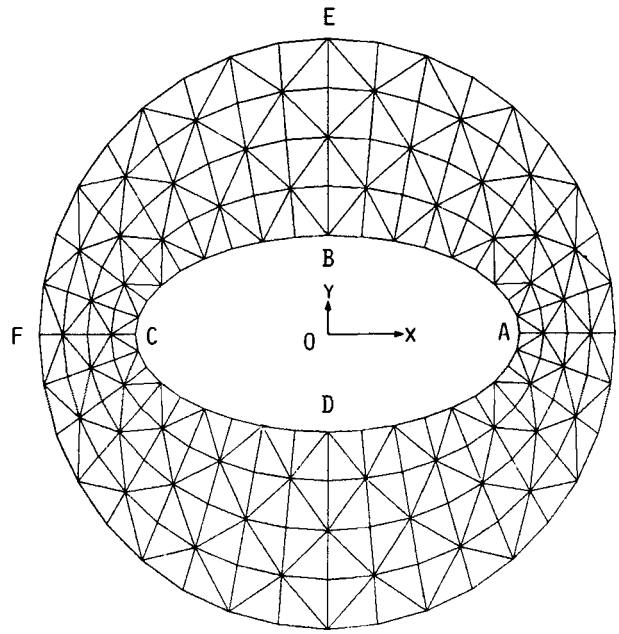

Figure 6. Finite element idealization for an elliptic island

in the formulation. The computed results obtained by the present method are in good agreement with the experimental and 3D boundary element solutions. The computational time for a single wave period was about 0·35 s using the HITAC M280H of the University of Tokyo. As reported in Yoshida and Ijima,[32] the 3D boundary element run required about 6 s computional time using the FACOM M200, which is a similar system. From this, it can be seen that the present method based on the mild-slope equation is effective for the analysis of surface waves on slowly varying water depth.

Finally, the present method is applied to a real port. For the numerical study, Sendai new port is chosen which is located on the northeastern side of Honshyu island, Japan. The port faces the Pacific ocean and the area is famous for the frequent occurrence of tsunami waves. Figures 13 and 14 show the finite element idealization and water depth diagram for Sendai new port. The total numbers of finite elements and nodal points are 497 and 318 respectively. The computed results of the relative wave amplitude at the points P and Q are compared with the observed results[33] versus

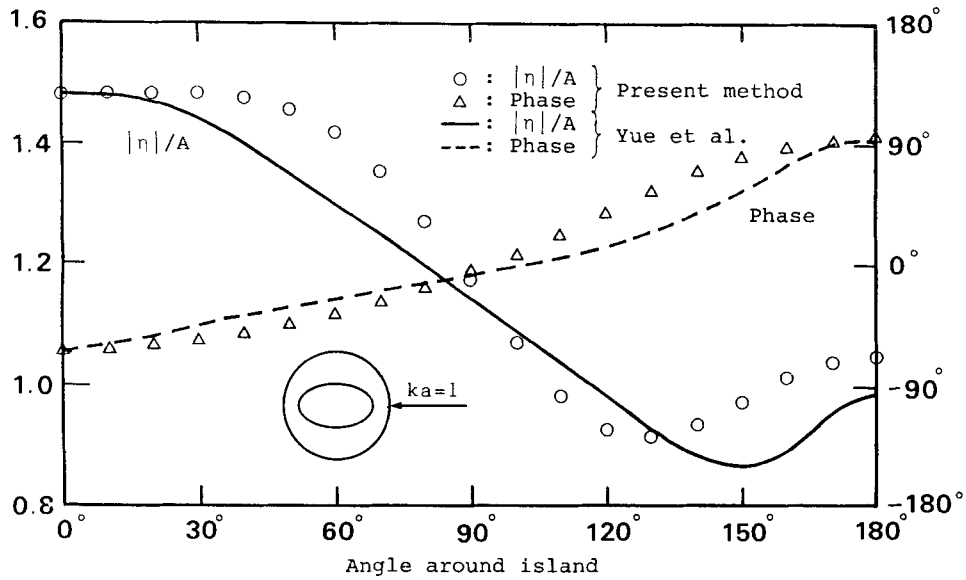

Figure 7. Computed relative wave amplitude and phase function when the incident wave angle is $\theta_{in} = 180°$

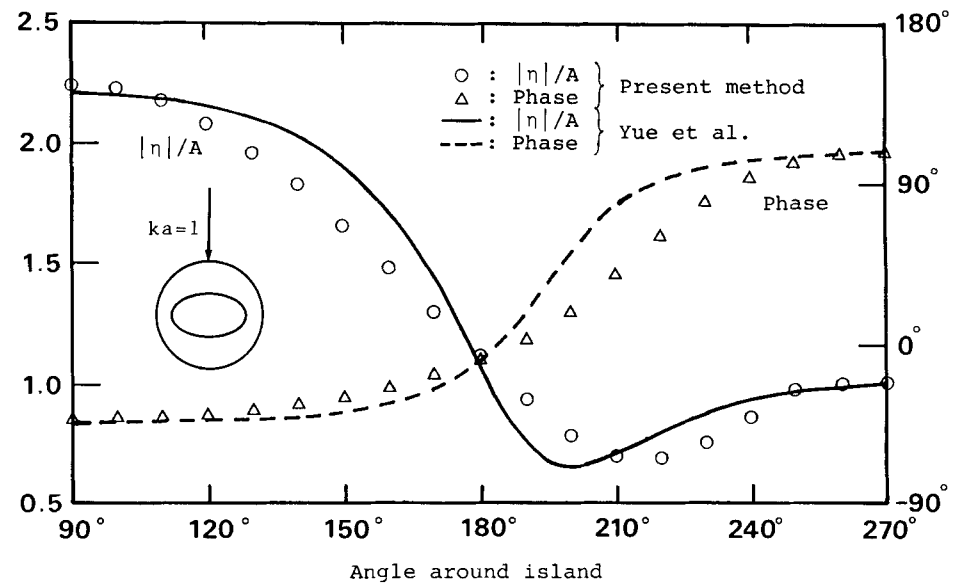

Figure 8. Computed relative wave amplitude and phase function when the incident wave angle is $\theta_{in} = 270°$

the incident wave period. The incident wave angle is assumed to be parallel to the breakwater, as shown in Figure 14. Figures 15 and 16 illustrate the comparison between computed and observed results. The abcissa represents the incident wave period and the ordinate is the relative wave amplitude. From these figures, it can be seen that the computed results obtained by the present method agree with the observed results.

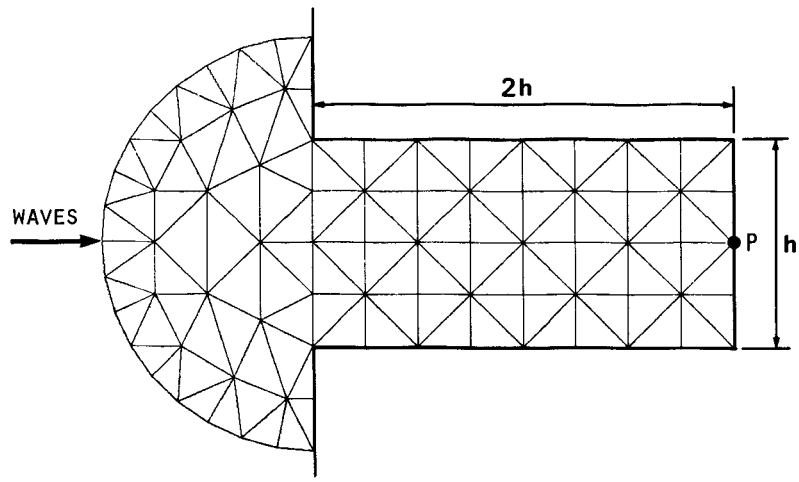

Figure 9. Finite element idealization for a rectangular harbour

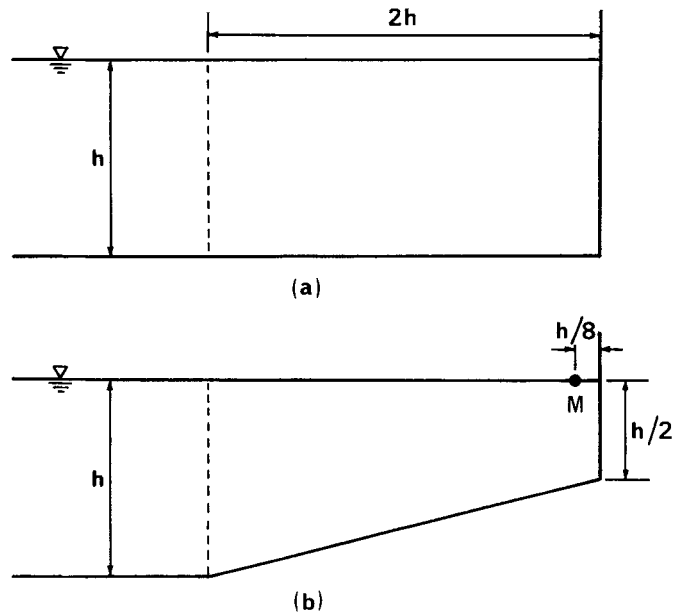

Figure 10. Water depth diagram for a rectangular harbour

CONCLUSION

A new combinative method based on the boundary-type finite element method has been presented to study water surface wave problems. The key features of this method are as follows. The variational function to be minimized can be formulated only by the line integral of an element, since the interpolation equation which satisfies the Helmholtz equation in each element is used in this paper. It follows that the discretized matrix equation can be formulated only by the calculation of a line integral. The boundary-type finite element is the C_0 non-conforming element; however, the computed results are in better agreement with the analytical solution than is the conventional combinative method using a conforming linear element. The convergence of the boundary-type

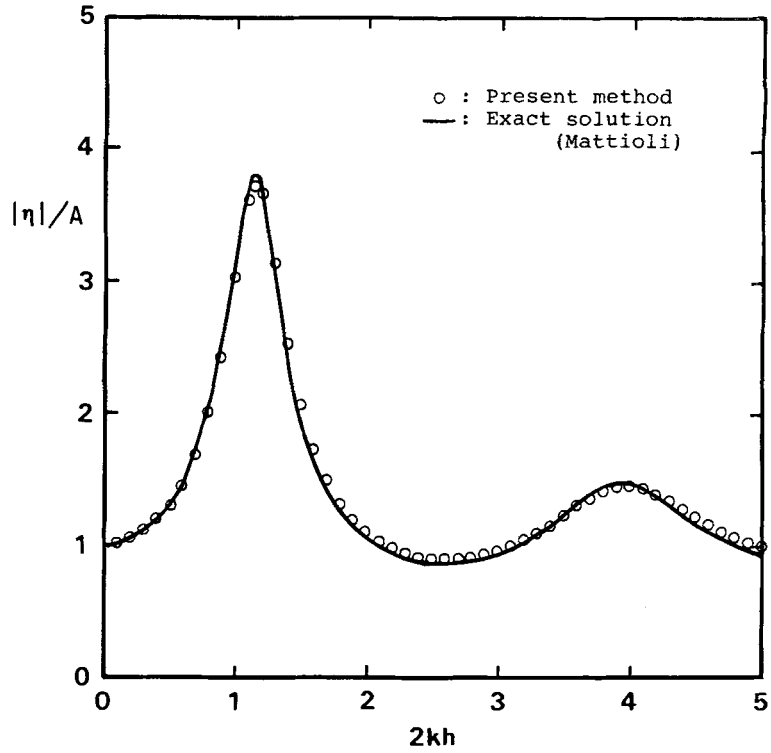

Figure 11. Computed relative wave amplitude at point P versus *kh*

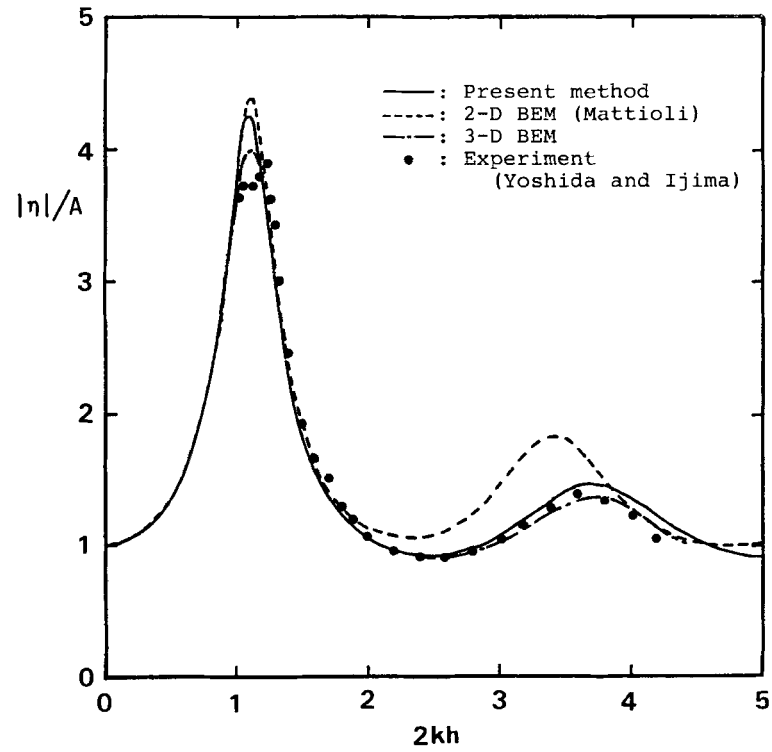

Figure 12. Comparison of relative wave amplitude at point P versus *kh*

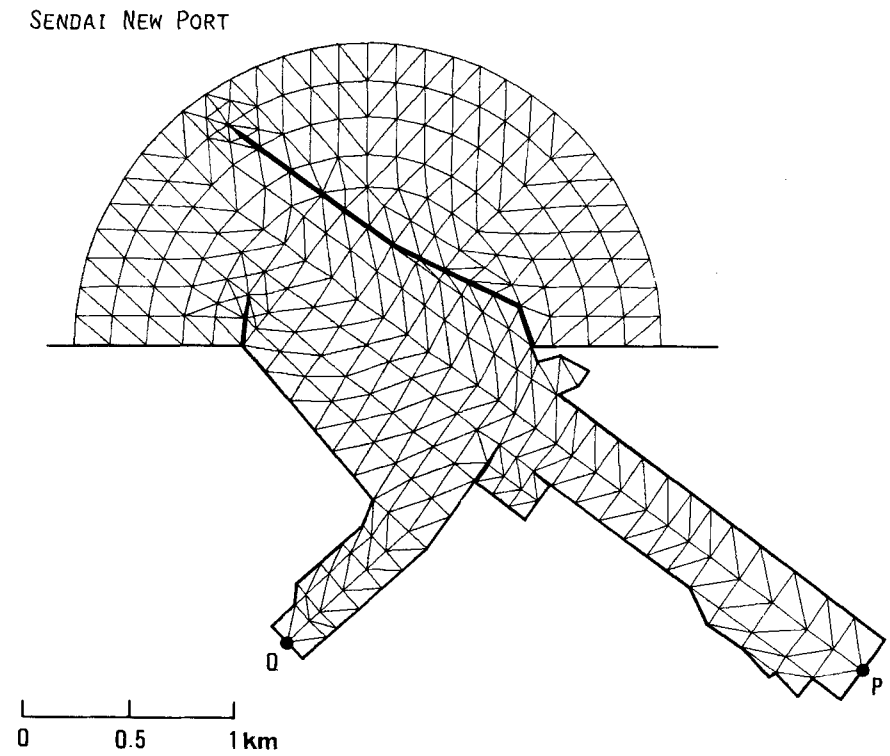

Figure 13. Finite element idealization for Sendia new port

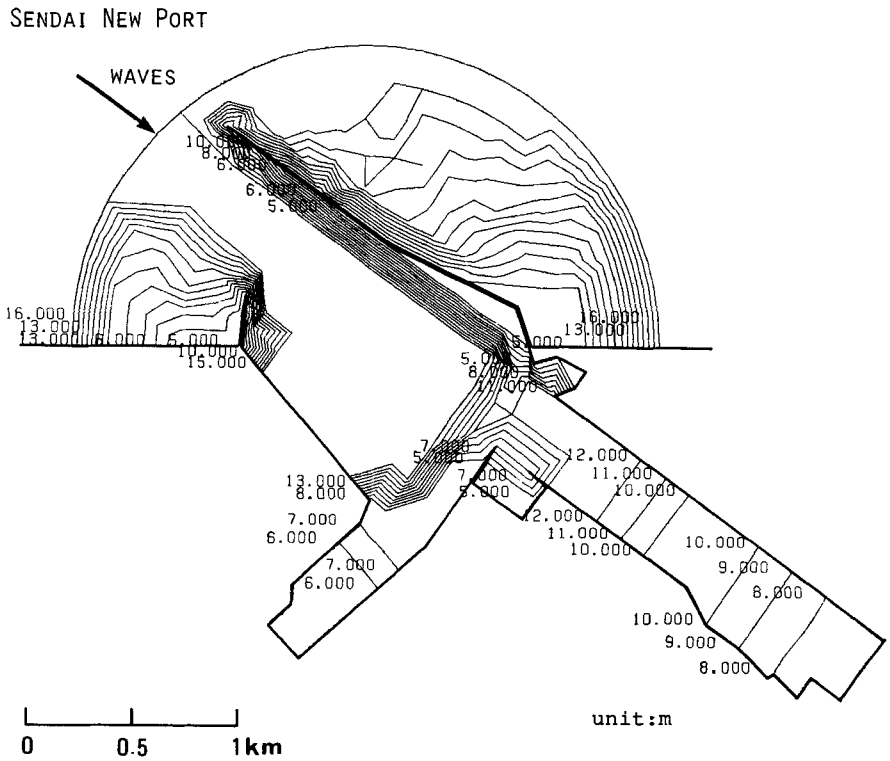

Figure 14. Water depth diagram for Sendia new port

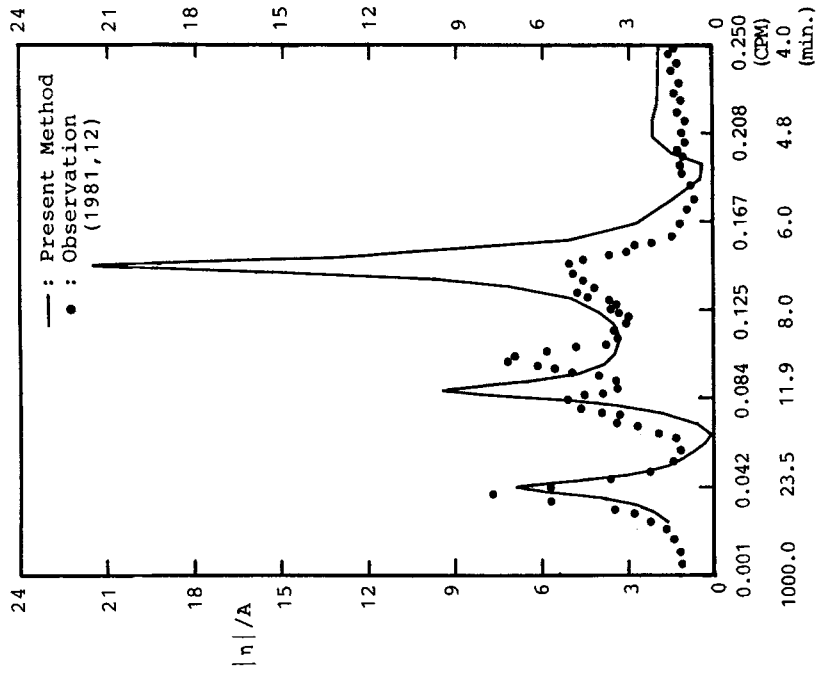

Figure 16. Comparison between computed and observed results at point Q

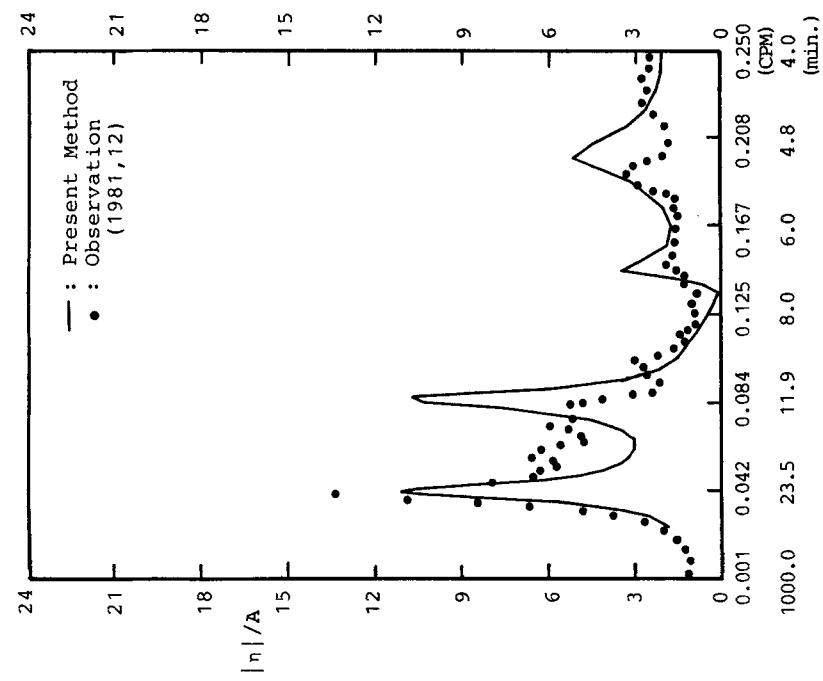

Figure 15. Comparison between computed and observed results at point P

finite element has been ensured by many numerical tests in References 22 and 23.

The computed results obtained by the present method have been compared with existing analytical, experimental, observed and other numerical results. From these comparative studies, it is concluded that the present method based on the mild-slope equation is a useful and effective tool for studying water surface wave problems.

ACKNOWLEDGEMENTS

The authors express their gratitude to Dr. Masaru Mizuguchi, Associate Professor of Chuo University, Dr. Tsukasa Nakayama, research associate of Chuo University, Mr. Hideyuki Sakurai, graduate student of Chuo University, and Mr. Yukio Aikawa, Unic Corporation, for their earnest discussions.

This research was supported in part by a Grand in Aid in Engineering and Science from the Ministry of Education of Japan.

REFERENCES

1. R. C. MacCamy and R. A. Fuchs, 'Wave forces on a pile: a diffraction theory', *Technical Memorandum No. 69*, U.S. Army Board, U.S. Army Corps of Engineering, 1954.
2. T. Kiyokawa, H. Kobayashi and M. Hino, 'Scattering of water waves and induced forces on vertical axisymmetric bodies', *Coastal Eng. Japan*, **26**, 175–192 (1983).
3. M. B. Abbott, H. M. Peterson and O. Skovgaard, 'On the numerical modelling of short waves in shallow water', *J. Hydraulic Res.*, **16**, 173–201 (1978).
4. C. Taylor, B. S. Patil and O. C. Zienkiewicz, 'Harbor oscillations: a numerical treatment for undamped natural modes', *Proc. Inst. Civil Eng.*, **43**, 141–155 (1969).
5. L. S. Hwang and E. O. Tuck, 'On the oscillations of harbors of arbitrary shape', *J. Fluid Mech.*, **43** (Part 3), 447–464 (1970).
6. J. J. Lee, 'Wave-induced oscillations in harbours of arbitrary geometry', *J. Fluid Mech.*, **45** (part 2), 375–394 (1971).
7. F. Mattioli, 'Wave induced oscillations in harbours of variable depth', *Comput. Fluids*, **6**, 161–172 (1978).
8. M. de St. Q. Isaacson, 'Vertical cylinders of arbitrary section in waves', *Proc. ASCE*, **104** (WW4), 309–324 (1978).
9. V. W. Harms, 'Diffraction of water waves by isolated structures', *Proc. ASCE*, **105** (WW2), 131–147 (1979).
10. H. S. Chen and C. C. Mei, 'Oscillations and wave forces in an offshore harbour', *Report No. 190*, Ralph M. Persons Lab., MIT, 1974.
11. O. C. Zienkiewicz, D. W. Kelly and P. Bettess, 'The coupling of the finite element method and boundary solution procedures', *Int. j. numer. methods eng.*, **11**, 355–375 (1977).
12. J. R. Houston, 'Combined refraction and diffraction of short waves using the finite element method', *Appl. Ocean Res.*, **3**, 163–170 (1981).
13. T. K. Tsay and P. L-F. Liu, 'A finite element model for wave refraction and diffraction', *Appl. Ocean Res.*, **5**, 30–37 (1983).
14. O. Skovgaard, L. Behrendt and I. G. Jonsson, 'A finite element model for wave diffraction', *Proc. 19th Int. Conf. on Coastal Engineering*, ASCE, 1984, pp. 1091–1102.
15. J. C. W. Berkhoff, 'Computation of combined refraction–diffraction', *Proc. 13th Int. Conf. on Coastal Engineering*, ASCE, 1972, pp. 471–490.
16. J. C. W. Berkhoff, 'Mathematical models for simple harmonic linear water waves, wave diffraction and refraction', *Report No. 163*, Delft Hydraulic Lab., 1976.
17. O. C. Zienkiewicz, D. W. Kelly, and P. Bettess, 'Marriage a la mode—The best of both worlds (finite elements and boundary integrals)', in R. Glowinsky, E. Y. Rodin and O. C. Zienkiewicz (eds), *Energy Methods in Finite Element Analysis*, Wiley, New York, 1977, pp. 81–107.
18. P. Bettess and O. C. Zienkiewicz, 'Diffraction and refraction of surface waves using finite and infinite elements', *Int. j. numer. methods eng.*, **11**, 1271–1290 (1977).
19. P. Bettess, C. Emson and T. C. Chiam, 'A new mapped infinite element for exterior wave problems', in R. W. Lewis, P. Bettess and E. Hinton (eds), *Numerical Methods in Coupled System*, Wiley, New York, 1984, pp. 489–504.
20. P. Bettess, S. C. Liang and J. A. Bettess, 'Diffraction of waves by semi-infinite breakwater using finite and infinite elements', *Int. j. numer. methods fluids*, **4**, 813–832 (1984).
21. O. C. Zienkiewicz, K. Bando, P. Bettess, C. Emson and T. C. Chiam, 'Mapped infinite elements for exterior wave problems', *Int. j. numer. methods eng.*, **21**, 1229–1251 (1985).
22. M. Kawahara and K. Kashiyama, 'Boundary type finite element method for surface wave motion based on trigonometric function interpolation', *Int. j. numer. methods eng.*, **21**, 1833–1852 (1985).

23. K. Kashiyama and M. Kawahara, 'Boundary type finite element method for surface wave problems', *Proc. JSCE*, No. 363/2, 205–214 (1985).
24. M. Kawahara, H. Sakurai and K. Kashiyama, 'Boundary type finite element method for wave propagation analysis', *Int. j. numer. methods fluids*, (in press).
25. R. Smith and T. Sprinks, 'Scattering of surface waves by a conical island', *J. Fluid Mech.*, **72** (part 2), 373–384 (1975).
26. C. C. Mei, *The Applied Dynamics of Ocean Surface Waves*, Wiley, New York, 1983.
27. N. Booij, 'A note on the accuracy of the mild-slope equation', *Coastal Eng.*, **7**, 191–208 (1983).
28. S. Homma, 'On the behaviour of seismic sea waves around circular island', *Geophys. Mag.*, **21**, 199–208 (1950).
29. A. C. Vastano and R. O. Reid, 'Tsunami response for islands: verification of a numerical procedures', *J. Marine Res.*, **25**, 219–235 (1967).
30. I. G. Jansson, O. Skovgaard and O. Brink-Kjaer, 'Diffraction and refraction calculations for waves incident on an island', *J. Marine Res.*, **34**, 469–496 (1976).
31. D. K. P. Yue, H. S. Chen and C. C. Mei, 'Water wave forces on three-dimensional bodies by a hybrid element method', *Report No. 215*, Ralph M. Persons Lab., MIT, 1976.
32. A. Yoshida and T. Ijima, 'Resonance in harbours of arbitrary topography', *Proc. 5th Int. Conf. on Boundary Elements*, 1983, pp. 217–226.
33. T. Fukute, K. Katahira, S. Matsui, S. Suzuki and T. Endow, 'Studies on observation and analysis of long waves', *Proc. 31st Japanese Conf. on Coastal Engineering*, 1984, pp. 198–202 (in Japanese).